

# Electrostatic Control of Intramolecular Electron Transfer in Calix[4]diquinones Bearing an Appended Chromophore\*\*

Muriel Hissler, Anthony Harriman,\* Pierre Jost, Georges Wipff, and Raymond Ziessel\*

Electron transfer is one of the few processes that can compete with deactivation of a short-lived excited state, and this facilitates construction of simple devices for use as chemosensors, for signal recognition, or for information processing.<sup>[1–3]</sup> Numerous studies have shown that the rate of electron transfer increases as the reactants approach each other, reaching a maximum at orbital contact.<sup>[4]</sup> Thus, when the redox units are located at the terminals of a flexible hydrocarbon chain, the rate of light-induced electron transfer depends on the molecular conformation,<sup>[5–7]</sup> being slowest for fully extended conformers. This realization, in turn, can be exploited to design a reversible optoelectronic switch, provided the conformation can be modulated by external stimulation. We now describe an example of such artificial tropism in which cation binding elongates a flexible molecule and, because electron transfer occurs preferentially in the closed conformer, restores luminescence from the appended chromophore.

Construction of a suitable system requires the cooperation of three discrete components, namely, an electron-rich chromophore, an electron acceptor, and a chelator, joined together by a flexible superstructure in such a way as to maintain the chelator between the redox-active units. Compounds **1** and **2**, calix[4]diquinones functionalized with a pendant 2,2'-bipyridine (bpy) unit and, respectively, [Ru<sup>II</sup>-(bpy)<sub>3</sub>] or *fac*-[Re<sup>I</sup>Cl(CO)<sub>3</sub>(bpy)] moieties, meet the essential

requirements. These compounds, together with the appropriate reference complexes **3** and **4**, were prepared by heating of the relevant ligand<sup>[8,9]</sup> at reflux with the precursor metal-fragment followed by column chromatography.

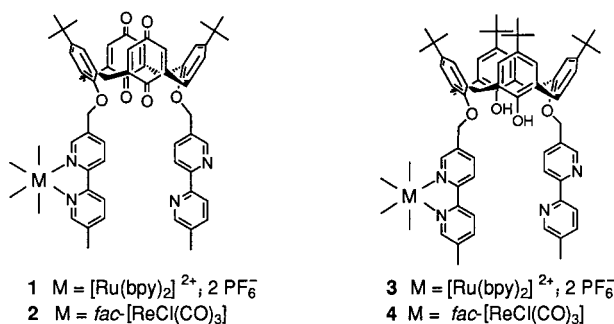
The *tert*-butyl groups impose a *syn* conformation for the podand bpy functionalities, but <sup>1</sup>H NMR studies of **1** and **2** indicate that the quinoid walls of the macrocyclic receptor rotate through the calixarene annulus at ambient temperature, a common situation for calix[4]diquinones.<sup>[10]</sup> The <sup>1</sup>H NMR spectrum of **3**, in particular, exhibits a well-defined AB quartet for each bridging methylene group of the calixarene platform and a single AB quartet for the oxy-methylene group next to the [Ru(bpy)<sub>3</sub>] moiety, and the cone conformation is also apparent from <sup>13</sup>C NMR spectra<sup>[11]</sup> ( $\delta = 34.0$  and  $33.9$  for the bridging methylene C atoms). The phenolic compounds **3** and **4** contain the chromophores but lack the electron-affinic quinoid units, while compound **2** is a neutral analogue of **1**.

Illumination of **3** or **4** in deoxygenated acetonitrile gave rise to phosphorescence with a maximum ( $\lambda_{\text{lum}}$ ) around 600 nm (Table 1). The excited triplet states of these reference com-

Table 1. Photophysical and electrochemical properties of **1–4** in deoxygenated acetonitrile at 20 °C.

Compd	$\lambda_{\text{lum}}$ [nm] <sup>[a]</sup>	$\Phi_{\text{lum}}$ <sup>[b]</sup>	$\tau_T$ [ns] <sup>[c]</sup>	$E_{\text{red}}$ <sup>[d]</sup>	$E_{\text{ox}}$ <sup>[e]</sup>	$\Delta G^\circ$ [eV] <sup>[f]</sup>
<b>1</b>	630	0.0004	6	−0.73 (72)	1.22 (72)	−0.26
<b>1</b> · Ba <sup>2+</sup>	635	0.057	740	−0.59 (irr.)	–	−0.31
<b>2</b>	610	0.0004	5	−0.75 (89)	1.32 (irr.)	−0.28
<b>2</b> · Ba <sup>2+</sup>	610	< 0.0001	0.085	−0.15 (irr.)	–	−0.78
<b>3</b>	625	0.085	1100	−1.43 (80)	1.35 (70)	> 0.6
<b>4</b>	615	0.0030	45	−1.35 (89)	1.36 (irr.)	> 0.6

[a] Phosphorescence maximum,  $\pm 5$  nm. [b] Emission quantum yield,  $\pm 15\%$ . [c] Triplet lifetime,  $\pm 5\%$ . [d] Reduction potential [V vs. SCE],  $\pm 15$  mV, measured with ferrocene as internal standard ( $E_{\text{red}} = 0.32$  V vs. SCE,  $\Delta E_p = 64$  mV). The splitting between anodic and cathodic peaks is given in parenthesis; irr. indicates irreversible. [e] Reduction potential for oxidation of the metal center [V vs. SCE],  $\pm 15$  mV. [f] Thermodynamic driving force for light-induced electron transfer,  $\pm 0.05$  eV.



[\*] Prof. A. Harriman, Dr. R. Ziessel, M. Hissler  
 Laboratoire de Chimie, d'Electronique  
 et Photonique Moléculaires  
 Ecole Européenne de Chimie  
 Polymères et Matériaux (ECPM)  
 Université Louis Pasteur  
 1 rue Blaise Pascal, 67008 Strasbourg Cedex (France)  
 Fax: (+33) 388-41-68-25  
 E-mail: harriman@chimie.u-strasbg.fr  
 ziessel@chimie.u-strasbg.fr

Dr. P. Jost, Prof. G. Wipff  
 Laboratoire de Modélisation et Simulation Moléculaire  
 Institut Le Bel, Université Louis Pasteur, Strasbourg

[\*\*] This work was supported by the ECPM, the CNRS, and the Royal Society of London. We thank Johnson Matthey PLC for their generous loan of precious metal salts.

pounds decayed by first-order kinetics, allowing facile measurement of the triplet lifetime  $\tau_T$ . The total emission quantum yield  $\Phi_{\text{lum}}$  was determined by integration of the corrected luminescence spectrum. Phosphorescence from the calix[4]-diquinone-derived species **1** and **2** was barely detectable, and these triplet states were considerably shorter lived than those of the corresponding phenolic compounds (Table 1). Luminescence quenching in **1** and **2** can be attributed to light-induced electron transfer from the triplet state of the metal complex to a nearby quinone unit. The thermodynamic driving forces ( $\Delta G^\circ$ ) for these reactions can be estimated from cyclic voltammetry<sup>[12]</sup> and luminescence spectroscopy according to Equation (1);  $E_T$  is the triplet energy of the metal complex,  $\Delta Z$  is the difference in electronic charge between radical pair and initial reactants,  $\epsilon_s$  is the static dielectric constant of the solvent, and  $R$  is the distance separating the Ru<sup>II</sup> or Re<sup>I</sup> cation from the center of the quinone unit at the moment of electron transfer.

$$\Delta G^\circ = E_{\text{ox}} - E_{\text{red}} - E_T + \frac{\Delta Z e^2}{4\pi\epsilon_0\epsilon_s R} \quad (1)$$

For these calculations it is assumed that electron transfer takes place preferentially at orbital contact, so that  $R$  is assigned a tentative value of 8 Å. The terms  $E_{\text{ox}}$  and  $E_{\text{red}}$  refer to one-electron reduction potentials for the metal center and for the quinone unit, respectively (Table 1); where electrochemically irreversible couples were observed in the cyclic voltammograms, the peak potentials were used to estimate  $\Delta G^\circ$ . The derived  $\Delta G^\circ$  values are modest (Table 1) but, while not favoring rapid through-bond electron transfer between remote reactants, they are sufficient for fast electron transfer at orbital contact.<sup>[4]</sup>

Molecular dynamics (MD) simulations for **1** in acetonitrile indicate that the coordinated bpy ligands come into orbital contact with the quinoid walls of the macrocyclic receptor, the latter existing in a partial cone or 1,3-*alternate* conformation (Figure 1, top). Through-space electron transfer is favored over through-bond interactions by selective charge injection into the unsubstituted bpy units coordinated to the metal center at the triplet level and by the poor electronic properties of the connecting chain.<sup>[13]</sup> Furthermore, the MD simulations indicate the presence of conformations in which one of these

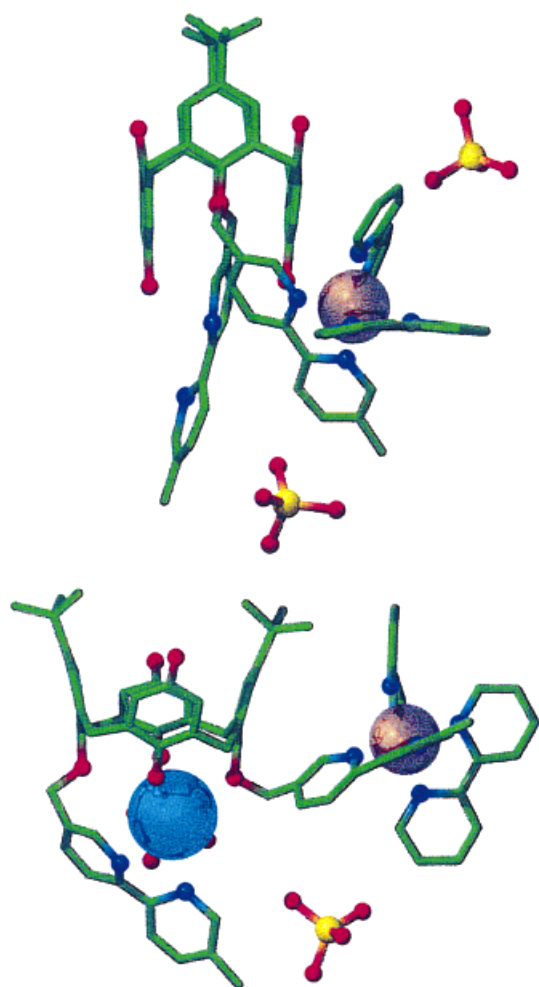


Figure 1. Energy-minimized conformations derived from molecular dynamics simulations for **1** (top) and **1**·Ba<sup>2+</sup> (bottom) in a matrix of acetonitrile molecules. Many different conformers are predicted to exist in dynamic equilibrium in the absence of added Ba<sup>2+</sup>, and the top structure corresponds to the conformation most favorable for rapid electron transfer.

parent bpy ligands lies almost cofacial and in very close proximity to a quinoid nucleus (Figure 1, top). Such structures are highly favorable for rapid (forward and reverse) electron transfer.<sup>[14]</sup> The electron-transfer pathway is less clear for **2**, where through-bond interactions might make some contribution to the overall process. Laser flash photolysis studies made for **1** and **2** with picosecond time resolution confirmed the short triplet lifetimes but could not resolve the anticipated redox products, indicating that the rate of charge recombination significantly exceeds that of charge separation.

Addition of a salt, such as KClO<sub>4</sub> or Ba(ClO<sub>4</sub>)<sub>2</sub>, to a solution of **3** or **4** in deoxygenated acetonitrile had no effect on the photophysical properties of the pendant metal complexes. For the rhenium(i) complex **2**, however, addition of salt caused extinction of residual phosphorescence, and in the presence of excess Ba(ClO<sub>4</sub>)<sub>2</sub> the triplet lifetime was reduced to 85 ± 5 ps. Furthermore, transient absorption spectra recorded after laser excitation of **2** ( $\lambda = 355$  nm, full width of half maximum height (FWHM) = 25 ps) in the presence of Ba(ClO<sub>4</sub>)<sub>2</sub> (5 mM) showed that the initially formed triplet state of the rhenium(i) complex decayed with a lifetime of about 90 ps to form a radical ion pair, which itself decayed by first-order kinetics with a lifetime of 175 ± 25 ps to restore the ground state. Generation of the radical ion pair, by way of intramolecular electron transfer from the triplet state of the rhenium(i) complex to a quinone unit, is promoted by barium cations because of a substantial increase in  $\Delta G^\circ$ . This arises because  $E_{\text{red}}$  (−0.75 V vs. SCE) is rendered less negative<sup>[12]</sup> by about 600 mV upon complexation of Ba(ClO<sub>4</sub>)<sub>2</sub> (Table 1). Consequently, the rate of intramolecular electron transfer ( $k_{\text{ET}} \approx 1.2 \times 10^{10} \text{ s}^{-1}$ ) derived according to Equation (2), where  $\tau_{\text{T}}^0$  and  $\tau_{\text{T}}^{\text{c}}$ , respectively, refer to triplet lifetimes measured

$$k_{\text{ET}} = \frac{1}{\tau_{\text{T}}^{\text{c}}} - \frac{1}{\tau_{\text{T}}^0} \quad (2)$$

for **2** in the presence of excess cation and for **4**, is increased 70-fold upon binding of the cation. Subsequent charge recombination ( $k_{\text{ET}} \approx 5.7 \times 10^9 \text{ s}^{-1}$ ) occurs more slowly, suggesting that this process occurs within the Marcus inverted region<sup>[15]</sup> because of the large amount of energy ( $\Delta G^\circ \approx -1.5 \text{ eV}$ ) that must be dissipated among vibrational modes.

Remarkably, addition of a cation to a solution of **1** in deoxygenated acetonitrile (Figure 2) caused a progressive increase in phosphorescence yield  $L$  until a plateau value was attained, at which the final luminescence yield  $L_\infty$  approached but never quite reached that measured for the phenol derivative ( $P^\circ$ ). Many different cations exhibit the same qualitative behavior (Table 2). In each case, the cation had little effect on the absorption spectrum of **1**, but the luminescence titration curve could be analyzed according to Equation (3);  $L_0$  is the luminescence yield in the absence of cation, and  $K$  is the binding constant for formation of a 1:1 complex.

$$\frac{1}{L_0 - L} = \frac{1}{L_0 - L_\infty} + \frac{1}{K[\text{cation}](L_0 - L_\infty)} \quad (3)$$

Time-resolved luminescence studies showed the presence of a long-lived species following addition of a cation; the

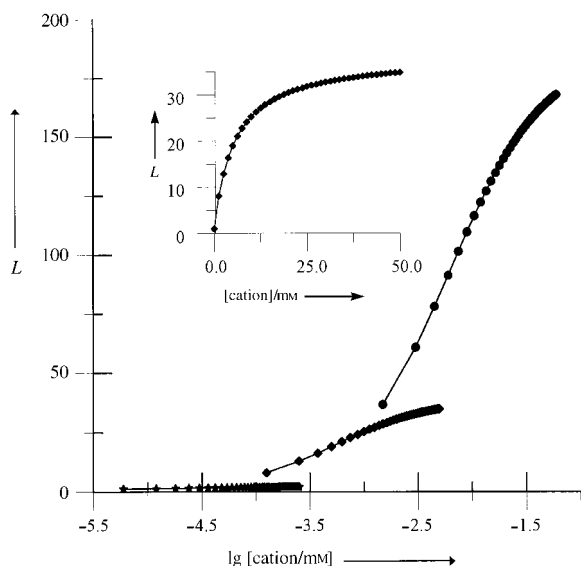


Figure 2. Effect of added  $\text{HClO}_4$  (\*),  $\text{KClO}_4$  (◆), and  $\text{Ba}(\text{ClO}_4)_2$  (●) on the phosphorescence yield  $L$  measured for **1** in deoxygenated acetonitrile containing  $0.2 \text{ M Bu}_4\text{NClO}_4$  at  $20^\circ\text{C}$ . The solid lines drawn through the data points correspond to nonlinear least-squares fits according to Equation (3) with the parameters listed in Table 2. The insert shows the titration curve recorded for addition of  $\text{KClO}_4$  in a nonlogarithmic presentation to illustrate attainment of a plateau.

Table 2. Properties of the 1:1 complexes formed between **1** and a cation at  $20^\circ\text{C}$  in deoxygenated acetonitrile containing  $0.2 \text{ M Bu}_4\text{NClO}_4$ .

Cation <sup>[a]</sup>	$K [\text{M}^{-1}]$ <sup>[b]</sup>	$\tau_T^\circ [\text{ns}]$ <sup>[c]</sup>	$L_\infty/P^\circ$ <sup>[d]</sup>	$k_{\text{ET}} [10^6 \text{ s}^{-1}]$ <sup>[e]</sup>
–	–	6	0.003	250
$\text{H}^+$	15850	9	0.008	110
$\text{Li}^+$	420	160	0.16	5.3
$\text{Na}^+$	400	160	0.15	5.3
$\text{K}^+$	185	155	0.14	5.5
$\text{H}_2\text{NH}^+$	160	130	0.10	6.8
$\text{Me}_4\text{N}^+$	8	210	0.21	3.9
$\text{Ca}^{2+}$	22	680	0.62	0.56
$\text{Ba}^{2+}$	16	740	0.67	0.44
$\text{Sr}^{2+}$	12	725	0.65	0.47
$\text{Cd}^{2+}$	30	720	0.66	0.48

[a] Used as the perchlorate salt, in some cases with water of hydration present. [b] Stability constant for formation of a 1:1 complex measured by steady-state luminescence spectroscopy,  $\pm 7\%$ . [c] Triplet lifetime for the cation complex,  $\pm 10\%$ . [d] Ratio of steady-state luminescence quantum yields measured for the cation complex of **1** and **3**,  $\pm 10\%$ . [e] Rate constant for intramolecular electron transfer in the cation complex,  $\pm 15\%$ .

measured triplet lifetime ( $\tau_T^\circ$ ) of this species approached that of **3** (Table 2). Clearly, complexation of a cation causes amplification of luminescence from the appended  $[\text{Ru}^{\text{II}}(\text{bpy})_3]$  complex, in contradiction to the situation found for **2**. With  $\text{Ba}(\text{ClO}_4)_2$  as the salt it was demonstrated that addition of excess [18]crown-6, a more avid cation complexer,<sup>[16]</sup> extinguished luminescence from **1**· $\text{Ba}^{2+}$  due to extraction of the cation.

The monocations are characterized by their relatively high binding constants and by their triplet lifetimes of about 150 ns, whereas the dications form less stable complexes with triplet lifetimes around 700 ns (Table 2). Protons bind avidly to the free bpy residue present in **1**, but have little effect on the

photophysical properties (Figure 2). Cyclic voltammetry studies carried out with **1** in acetonitrile showed that  $E_{\text{red}}$  for the quinoid moiety<sup>[12]</sup> was raised by about 140 mV upon coordination of barium cations such that  $\Delta G^\circ$  is increased slightly (Table 1). Clearly, the observed amplification of phosphorescence upon cation binding is contrary to the behavior expected on the basis of simple thermodynamic considerations.

Detailed  $^1\text{H}$  and  $^{13}\text{C}$  NMR studies and MD simulations of the complex with  $\text{Ba}(\text{ClO}_4)_2$  indicate that the cation binds to the lower rim of the calix[4]diquinone receptor,<sup>[17]</sup> where it is held in place by coordination to the four oxygen atoms and two nitrogen atoms provided by the free bpy ligand. The bound cation forces the macrocycle into a cone conformation and repels the appended  $[\text{Ru}^{\text{II}}(\text{bpy})_3]$  moiety (Figure 1, bottom). This has the effect of both curtailing orbital contact between the reactants and preventing adoption of the closely spaced cofacial orientations believed to favor fast electron transfer. From the MD simulations we estimate that the maximum edge-to-edge separation between quinone and bpy functionalities is about  $5 \text{ \AA}$ , so that one or more solvent molecules can fit between the reactants in the fully extended conformation (Figure 1). Given that the attenuation factor<sup>[4]</sup> for through-space electron tunnelling is around  $1.2 \text{ \AA}^{-1}$ , elongation of the supermolecule would cause a 650-fold decrease in the rate of electron transfer. Allowing for the crudity of this estimation, together with the fact that  $\Delta G^\circ$  increases upon cation binding and that there are changes in orientation as well as separation, the observed decrease in  $k_{\text{ET}}$  appears to be of the expected magnitude for through-space electron tunnelling.

Consequently, the dramatic drop in  $k_{\text{ET}}$  that accompanies cation binding to **1** can be attributed to an electrostatically driven conformational change that serves to separate the reactants and to force the calixarene into the cone conformation.<sup>[18–20]</sup> Amplification of emission depends only on the electronic charge of the cation, with  $k_{\text{ET}}$  remaining about 10-fold higher for a monocation than for a dication, although protons give an anomalously weak effect (Figure 2). The increase in luminescence is fully reversible, as illustrated in the top part of Figure 3 for the case of adding successive amounts of [18]crown-6 to the complex formed between **1** and  $\text{KClO}_4$ , with both complexation and decomplexation steps being fast. In fact, the bimolecular rate constant for complexation of  $\text{Sr}^{2+}$  by **1** in acetonitrile was measured by stopped-flow techniques to be around  $2 \times 10^5 \text{ M}^{-1} \text{ s}^{-1}$ , while subsequent decomplexation by [18]crown-6 occurred with a rate constant of about  $1 \times 10^5 \text{ M}^{-1} \text{ s}^{-1}$  (Figure 3, bottom).

## Experimental Section

The synthesis and characterization of complexes **1–4** will be described elsewhere. **1**: ES-MS ( $\text{CH}_3\text{CN}$ ):  $m/z$ : 1487.6  $[\text{M} - \text{PF}_6]^+$ , 671.1  $[\text{M} - 2\text{PF}_6]^{2+}$ ; FT-IR (KBr):  $\tilde{\nu} = 1654 \text{ cm}^{-1}$  (s, CO); UV/Vis ( $\text{CH}_3\text{CN}$ ):  $\lambda$  (ε) = 451 (14400), 288 (116500), 251 nm (81800); elemental analysis calcd for  $\text{C}_{80}\text{H}_{72}\text{F}_{12}\text{N}_8\text{O}_6\text{P}_2\text{Ru}$  ( $M_r = 1632.51$ ): C 58.86, H 4.45, N 6.86; found: C 58.70, H 4.23, N 6.75.

Luminescence lifetimes were measured by time-correlated, single-photon counting methodology following laser excitation at 440 nm and with detection at 620 nm. Laser flash photolysis studies were made by pump-

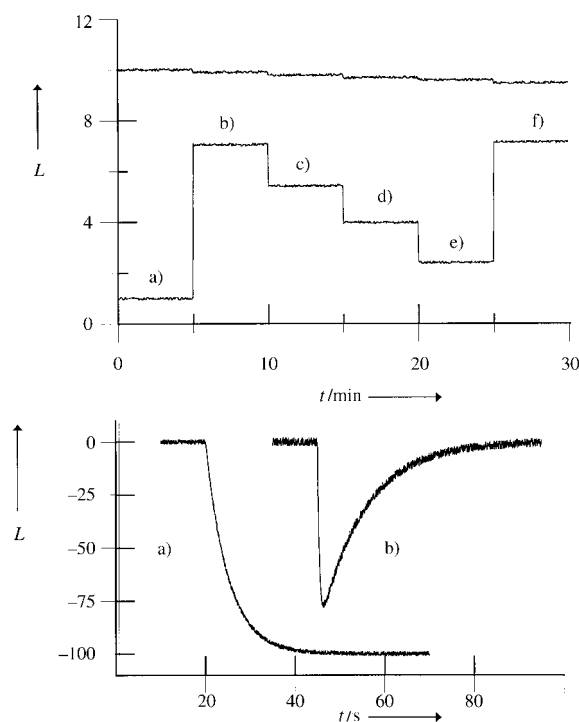


Figure 3. Top: The lower curve shows the phosphorescence intensity  $L$  recorded as a function of time  $t$  for  $20\ \mu\text{M}$  **1** in deoxygenated acetonitrile containing  $0.1\ \text{M}$   $\text{Bu}_4\text{NClO}_4$  a) before addition of a cation and b) upon addition of  $1\ \text{mM}$   $\text{KClO}_4$ ; c)–e) intensities after additions of  $0.3$ ,  $0.3$ , and  $0.4\ \text{mM}$  [18]crown-6; f) intensity after addition of further  $1\ \text{mM}$   $\text{KClO}_4$  to the mixture. The upper curve shows the corresponding experiment made for **3** and is uncorrected for the (minor) effects of dilution. Top: Kinetic experiment showing a) the rate of appearance of phosphorescence upon rapid injection of  $5\ \text{mM}$   $\text{Sr}(\text{ClO}_4)_2$  into a solution of **1** ( $10\ \mu\text{M}$ ) in deoxygenated acetonitrile containing  $0.1\ \text{M}$   $\text{Bu}_4\text{NClO}_4$  and b) decomplexation caused by injection of  $1\ \text{mM}$  [18]crown-6 to the solution.

probe techniques following excitation at  $355$  or  $440\ \text{nm}$  with a  $25\text{-ps}$  laser pulse. All studies were carried out with optically dilute solutions of the calix[4]arenes in deoxygenated acetonitrile. Binding constants were determined by monitoring absorption and/or luminescence spectral profiles as a function of cation concentration and using global analytical iterative routines provided by the SPECFIT commercial software. Rates of complexation and decomplexation were measured by stopped-flow techniques with luminescence detection at  $20^\circ\text{C}$  under pseudo-first-order conditions for solutions of  $\text{Bu}_4\text{NClO}_4$  ( $0.1\ \text{M}$ ) in acetonitrile. Molecular dynamics simulations were performed in acetonitrile with the AMBER4.0 software package for  $500\ \text{ps}$ . Interactions involving barium and ruthenium cations and all other nonbonding interactions are depicted by a  $1\text{--}6\text{--}12$  potential, where electrostatics are approximated by Coulombic forces, using atomic charges determined by ab initio calculation on the quinone, anisole, and  $[\text{Ru}(\text{bpy})_3]^{2+}$  molecular fragments. Reduction potentials were measured by cyclic voltammetry using Pt discs as working and counter electrodes and with an SCE reference calibrated versus ferrocene/ferrocium.

Received: June 8, 1998 [Z11956IE]

German version: *Angew. Chem.* **1998**, *110*, 3439–3443

**Keywords:** calixarenes • electron transfer • electrostatic interactions • luminescence • through-space interactions

- [1] A. W. Czarnik in *Fluorescent Chemosensors for Ion and Molecule Recognition* (Ed.: A. W. Czarnik), *ACS Symp. Ser.* **1992**, *538*, 1.
- [2] A. P. de Silva, H. Q. N. Gunaratne, T. Gunlaugsson, A. J. M. Huxley, C. P. McCoy, J. T. Rademacher, T. E. Rice, *Chem. Rev.* **1997**, *97*, 1515.

- [3] P. D. Beer, *Acc. Chem. Res.* **1998**, *31*, 71.
- [4] a) G. L. Closs, J. R. Miller, *Science* **1988**, *240*, 440; b) J. R. Miller, *Nouv. J. Chim.* **1987**, *11*, 83.
- [5] A. Harriman, *Pure Appl. Chem.* **1990**, *62*, 1107.
- [6] M. T. Indelli, C. A. Bignozzi, A. Harriman, J. R. Schoonover, F. Scandola, *J. Am. Chem. Soc.* **1994**, *116*, 3768.
- [7] D. Goztola, B. Wang, M. R. Wasielewski, *J. Photochem. Photobiol. A* **1996**, *102*, 71.
- [8] G. Ulrich, R. Ziessel, *Tetrahedron Lett.* **1994**, *35*, 6299.
- [9] H. Cano-Yelo Bettega, J.-C. Moutet, G. Ulrich, R. Ziessel, *J. Electroanal. Chem.* **1996**, *406*, 247.
- [10] A. Casnati, E. Cornelli, M. Fabbri, V. Bocchi, G. Mori, F. Ugozzoli, A. M. Manotti-Lanfredi, A. Pochini, R. Ungaro, *Recl. Trav. Chim. Pays-Bas* **1993**, *112*, 384.
- [11] C. Jamie, J. de Mendoza, P. Prados, P. M. Nieto, C. Sánchez, *J. Org. Chem.* **1991**, *56*, 3372.
- [12] Reduction of a calix[4]diquinone without an appended metal complex occurs by four successive one-electron steps, by which the two  $\pi$  radical anions are formed before the  $\pi$  dianions. The electrochemical inequivalence of the quinoid units arises from Coulombic effects. Addition of  $\text{Ba}(\text{ClO}_4)_2$  removes the Coulombic effect, at least for formation of the  $\pi$  radical anions, and stabilizes the emergent negative charge by ion pairing. This stabilization amounts to about  $490\ \text{meV}$  and corresponds to the difference in stability constant for cation binding to the quinones and their  $\pi$  radical anions. In the presence of excess cation, the reductive process is electrochemically irreversible, whilst ion pairing might involve the bound cation or a second cation from solution. Similar behavior is found for **1** except that the shift in potential is decreased to around  $140\ \text{meV}$ . This latter finding suggests a much smaller change in the stability constant on going from the quinone to the  $\pi$  radical anion, presumably because the quinone O atoms are already involved in complexation and/or the dicationic donor inhibits secondary ion pairing. For **2**, stabilization of the  $\pi$  radical anions by  $\text{Ba}(\text{ClO}_4)_2$  corresponds to about  $600\ \text{meV}$ , suggesting that the dominant mode of ion pairing involves a second cation from the solution.
- [13] A. C. Benniston, A. Harriman, V. Grossshenny, R. Ziessel, *New J. Chem.* **1997**, *21*, 405.
- [14] B. Brocklehurst, *J. Phys. Chem.* **1979**, *83*, 536.
- [15] R. A. Marcus, N. Sutin, *Biochim. Biophys. Acta* **1985**, *811*, 265.
- [16] a) K. Ozutsumi, K. Kohyama, K. Ohtsu, T. Kawashima, *J. Chem. Soc. Dalton Trans.* **1995**, 3081; b) quantitative analysis of the fluorescence titration (a part is displayed in Figure 3a) gives  $\lg K = 4.26$  for complexation of  $\text{K}^+$  by [18]crown-6 under these conditions.
- [17] P. D. Beer, P. A. Gale, Z. Chen, M. G. B. Drew, J. A. Heath, M. I. Ogden, H. R. Powell, *Inorg. Chem.* **1997**, *36*, 5880.
- [18] S. Shinkai, S. Araki, M. Kubota, T. Arimura, T. Matsuda, *J. Org. Chem.* **1991**, *56*, 295.
- [19] J. Blixit, C. Detellier, *J. Am. Chem. Soc.* **1995**, *117*, 8536.
- [20] M. Gomez-Kaifer, P. A. Reddy, C. D. Gutsche, L. Echegoyen, *J. Am. Chem. Soc.* **1997**, *119*, 5222.